

Original Research Article

Using safe calculated low power of electrons to cut, analyze and exterminate the outer and inner biological elements of SARS-CoV-2, MERS-CoV-2 and Influenza viruses in vitro

Abstract

Background: The treatment of pneumonia viruses with antiviral drugs produced mild to severe side effects until the immune system **worked against** the invaded virus.

Objective: Therefore, it is crucial to develop **an** efficient alternative therapy with lower side effects against infection of pneumonia viruses.

Methods: We hereby designated a novel device termed **a a Life** Restoration Device (LRD) to produce electric frequencies with lower potential. The electric **frequencies can** specifically destroy the nucleic acid materials and viral envelope rather **than the plasma** of the infected cell. Using a glass tube model the infected cells with propagated viruses were filled in the glass tube and two nickel-coated copper rods were inserted **into** both ends. Then the two rods were connected into the LRD. Lower potential electric frequencies were applied for 30 min and 60 min **onto the infected cells**.

Results: The treatment of the infected cell culture of MERS-CoV and SARS-CoV-2 using LRD for 30 min significantly reduced the viral infectivity **to 83%** and 22% respectively. After 60 min of MERS-CoV and SARS-CoV-2 exposure **to LRD**, the infectivity **reduced to** 21% and 1% respectively. Additionally, based on the data of transmission electron microscopy **of the H5N1 virus** and electrophoretic patterns of different types of viruses, the nucleic acid materials of the treated viruses were reduced based on the non-treated viruses. The electric frequencies sensitivity produced by LRD can reduce the fluidity of **the viral envelope** rather than **the plasma** membrane of the infected cells.

Conclusion: Treatment of pneumonia viruses with electric stimulation is a new alternative therapy but needs more investigations. The data obtained from this study is important to develop an effective alternative viral therapy.

Keywords: Life Restoration Device, codified number of ions, human viruses, MERS-CoV, SARS-CoV-2, Influenza viruses, viral extermination

1. Introduction

Viruses are tiny infectious intracellular microorganisms with genetic materials (DNA or RNA).¹ Many viruses can infect the respiratory, tracts and cause serious disorders.² Recently, respiratory tract viral infection considers a big dilemma.³ For example influenza A virus subtype (H5N1) and severe acute respiratory syndrome (SARS) coronavirus are pathogens that cause severe viral pneumonia that causes a higher mortality rate.^{4,5} Interestingly the World Health Organization (WHO) has directed their interests about the viral potential pandemic with the threat to humans.^{4,6}

Until now, there isn't a clear strategy to protect or prevent the coronavirus disease (COVID-19) pandemic. The COVID-19 pandemic is a serious sickness caused by Severe Acute Respiratory Syndrome Coronavirus 2 (SARS-CoV-2). The symptoms of the illness range from asymptomatic, mild, or severe respiratory symptoms.⁷ In October 2018, more than 2260 cases of confirmed MERS-CoV infection and 803 related deaths have been reported.⁸ Moreover, different subtypes of coxsackievirus such as type A9 (COX A9) virus can cause severe symptoms such as hepatitis and encephalitis [9]. Additionally, herpes simplex type 1 (HSV1) may produce causes orolabial disease and genital and newborn infections.¹⁰

Notably, different treatment strategies against respiratory viral infections were developed. For example, vaccination is the most effective and cheap method to protect from pneumonia and respiratory viral infections. In the coming decades, it is hoped that pneumonia vaccines will give effective and universal protection, and that developed vaccines will be important for other causes of viral pneumonia.¹¹ However, it is clear that protection from viral infection using vaccination is not effective and takes a long time to get the desired protection rate. Another type of treatment of the

viral infection is using antiviral drugs. It is well known that chronic hepatitis B can be treated using interferon or a combination of nucleoside analogs.¹² Unfortunately, the treatment with antiviral drugs produced severe side effects for long time course treatment. Additionally, the inactivation of many non-enveloped and enveloped pathogens by treatment with higher intensity of broad-spectrum pulsed light (Pure Bright) has been studied. Interestingly, a comparison of ultraviolet irradiation showed that lower wavelength particularly inactivates non-enveloped viruses.^{13,14} Notably, this type of non-invasive or alternative therapy of viral infection is relatively preferable because it is characterized by low cost, safe, low side effects and effectiveness.

Recently, the use of non-invasive and alternative therapy against viral infection is more effective, painless and safe. For example, human immunodeficiency virus type 1 (HIV-1) endocytosed by cells is damaged by direct or indirect application of electric stimulations, resulting in a reduction of HIV-1 infectivity.^{15,16,17} Interestingly, it was suggested that the controlled electric impulses stimulation can improve respiratory functions, inhibit SARS-CoV-2 infectivity, reduce pain, improve immunity and increase the efficacy of antiviral drugs.¹⁸

Therefore, in this study, we designed a small device, called Life Restoration Device (LRD). The LRD was registered in the Patent Office, Ministry of Higher Education, Academy of Scientific Research and Technology, Cairo, Egypt and has a patent number: 2014101664/2014/10/20. The LRD is able to destroy several types of viruses especially those infecting the respiratory tract. The scientific base of the LRD function is the electronic transformation of low voltage electric impulses into codified energy with specific characterizations. The codified energy is coded to destroy the biological contents of viruses such as RNA/DNA. In vitro treatment of some respiratory viruses such as H5N1, SARS-CoV-2 and MERS-CoV with LRD significantly reduced the viral load in a short time. The data obtained from this study will introduce important information in

the non-invasive and alternative therapy of serious respiratory virus infection. The short time treatment of the viral infection with LRD might reduce symptoms and side effects of respiratory virus infection.

2. Material and Methods

2.1. Materials

Avian influenza RGA/Chicken/Egypt/813825A/2017 virus (H5N1), coronavirus 2 or SARS-CoV-2 (COVID-19) and Middle East respiratory syndrome coronavirus (MERS-CoV), coxsackievirus type A9 (COX A9) virus, herpes simplex type 1 (HSV1) were purchased from European virus archive-global (Marseille, France). African green monkey kidney, (VERO-CCL-81) cell line and Madin-Derby Canine Kidney (MOCK) cell line were obtained from the American Type Culture Collection, (Rockville, Md, USA). Dulbecco's modified Eagle medium (DMEM) supplemented with 8% fetal bovine serum and 1% antibiotic-antimycotic mixture was purchased from BioWhittaker (Walkersville, MD, USA). Precast gradient NuPAGE Novex 4-12% Bis-Tris protein gels and Page Ruler Prestained Protein Ladder were obtained from Invitrogen, Thermo Fisher Scientific, Inc. (Dreieich, Germany). Beta-mercaptoethanol, crystal violet, agarose and silver nitrate solution were obtained from Sigma-Aldrich Chemie GmbH (Taufkirchen, Germany).

2.2. Tested viruses

The *in vitro* studies were performed to provide more information about the effect of the produced low potential codified number of ions from LRD on different types of respiratory viruses. For example, H5N1, COVID-19, MERS-CoV and HSV1 were used as representatives for enveloped RNA viruses. While COX-A9 virus was used as a non-enveloped RNA virus.

2.3. Cell cultures

African Green Monkey Kidney, (VERO-CCL-81) cell line for cultivation and breeding of MERS-CoV and SARS-CoV-2. Furthermore, Madin-Derby Canine Kidney (MOCK) cell line was used to maintain and seed H5N1.

3. Methods

3.1. LRD design for in vitro experiment

As shown in Figure 1 the designed glass tube was filled with cell medium and targeted virus. Hereafter, the nickel-coated copper rod connected with a rubber plug was inserted in each side of the glass tube. The codified number of ions produced from the LRD was applied at different time points (30 min and 60 min). Then the treated and non-treated viruses were analyzed and propagated for further analysis.

3.2. Experimental system design

As shown in Figure 2, the propagated viruses in the specified cell line and culture medium were poured into the designed glass tube. Both input and output plugs connected with nickel-coated copper rods were plugged into each side of the glass tube. Each side of the glass tube was firmly sealed to prevent the leakage of the cell line medium.

Hereafter, each side of the nickel-coated copper rod was connected with the LRD. The low potential electrical frequencies were codified into the number of ions and the treatment with LRD was applied for 30 min and 60 min.

3.3. Virus preparation and system assembly

Viruses were diluted in 12 ml (DMEM supplemented with 2% fetal bovine serum and 1% antibiotic-antimycotic mixture and poured into the system. Control (untreated) virus solution was kept in the same exposure time and then stored at -70 °C. The diluted viruses were exposed to LRD for

30 min and 60 min and the virus was withdrawn, aliquoted and stored in a -70 °C freezer.

3.4. Cell culture preparation

The MDCK or VERO cells in 75 cm² tissue culture flasks were treated with trypsin for cell dissociation and re-suspended to give 10⁵ cells/ml in DMEM. Suspended cells were cultivated in six-well tissue culture plates and incubated for 24 hrs- at 37 °C.

3.5. Virus propagation

Viruses were propagated based on the previously published methods with some modifications.^{19,20} The titration for MERS-CoV, SARS-CoV-2 H5N1, HSV1 and COX-A9 viruses and plaque infectivity assay was carried out. Briefly, the propagated viruses were 10 folds serially diluted in a DMEM medium without FBS. Then, 100 µl of each dilution was mixed with 200 µl of infection medium and used to inoculate 80-90% confluent VERO-E6 for infectivity assay test of MERS-CoV or SARS-CoV-2 or COX-A9 and MOCK cells for infectivity assay test of H5N1 and HSV1 viruses. Control was included in the plate that was inoculated with 300 µl of serum-free medium. The plate was incubated at 37 °C under 5% CO₂ for 1 h to allow virus adsorption and rocked every 15 min to ensure homogenous exposure of the cells to infection and avoid drying of cells. After 1 h, 3 ml of the over-layer medium were added, and the plate was agitated to allow homogenous mixing of the virus inoculum through the over-layer. To allow the solidification of the agarose component of the over-layer medium, the plate was left at room temperature for about 10 min then further incubated at 37 °C under 5% CO₂. After 72 h, 1 ml of fixation solution was added to each well for 1 h for cell fixation and virus inactivation.

3.6. Plaque infectivity reduction assay

The assay was carried out according to the method of Hayden et al. (1980). The growth medium was removed from the cell culture plates and treated viruses were inoculated (100 µl/well) into the prepared cell culture six-well plates. After 1 h contact time for virus adsorption, 3ml of DMEM supplemented with 2% agarose was added onto the cell monolayer and plates were left to solidify and incubated at 37 °C till the formation of viral plaques (3 to 4 days). Control cells (untreated viruses) were **treated similarly**. Plaques were counted **under the microscope** and percentage reduction in the formation of plaques in comparison to control wells was calculated as **follows**: [% inhibition = viral count (untreated) – viral count (treated)/viral count (untreated) **x 100**]. All experiments were carried out three times for confirmation.^{21,22}

After LRD treatment, for visualization of the plaques, formalin (10%) was added for two hours for cell fixation then plates were stained with 0.1 % crystal violet in distilled water for 5 min. Then dye was discarded, plate wells were rinsed in water and dried. Viral plaques were evidenced as clear unstained spots (due to viral infection) in a violet (stained cells) background. Then the virus titer was calculated through the following equation: Plaque forming unit (PFU)/ml = Number of plaques x inoculated volume of the virus x virus dilution x 10.

3.7. The role of LRD rod type and viral load inhibition

Nevertheless, to make sure that the anti-SARS-CoV-2 activity was due to the applied codified **number of ions** and not due to the chemical precipitate or type of the metal rode used in the LRD. Therefore, we applied a codified **number of ions** to the media with the virus through two different metal rode (nickel-coated copper rod and nickel-coated iron rod). Hereafter the viral load inhibition and the antiviral activity of the precipitate formed against SARS-CoV-2 were evaluated.

3.8. Viral genome examination

All treated and untreated viruses were extracted for their nucleic acids and PCR and RT-PCR were carried out to determine any effect on virus nucleic acids. The PCR amplicons were separated individually on 1% agarose gel.

3.9. Sodium dodecyl sulfate polyacrylamide gel electrophoresis (SDS-PAGE)

Normalized protein samples (after determining the protein concentration) were mixed with 4x "Laemmli buffer" containing 10% beta-mercaptoethanol to reduce disulfide bonds. The mixture was then incubated at 95 °C for 5 min, cooled on ice for 1 min and shortly centrifuged. Afterward, 10 µl of each sample was then resolved on "precast gradient NuPAGE Novex 4-12% Bis-Tris protein gels" (Invitrogen, Germany) using "XCell Surelock Mini-Cell electrophoresis system" (Invitrogen). **Page Ruler** Prestained Protein Ladder (Thermo) was loaded as a marker. "1x NuPAGE MOPS/SOS running buffer" was added to the chamber, a cover was placed over the electrophoresis unit and the electric current was set at 150 V.²³

3.10. Silver staining

The gel was soaked in a fixation solution for 1 h while shaking at 37 °C. The gel was then soaked for 30 min in conditioner solution while shaking at 37 °C. Then it was washed 3 times each for 5 min with distilled water while shaking. Hereafter silver nitrate stain solution was applied for 20 min while shaking. The gel was washed 2 times each for 10 sec in distilled water. For visualizing the stained bands, the gel was soaked in the developer and the development of the brown bands was carefully observed. To avoid darkening of the background the reaction was stopped by soaking the gel in the stopping solution.²³

3.11. Electrophoretic pattern

In the electrophoretic pattern experiment; 2ml of each treated virus and untreated controls were concentrated in 50 KDa cut-off Millipore concentration falcon tubes. The concentrated viruses were **electrophoretically** separated on 10-12% gradient SDS-polyacrylamide gel and stained with silver stain.

3.12. Viral genome examination

For viral genome examination, RT-PCR and PCR will be carried out for full-length influenza genome segments and to specific regions in the virus genome of SARS-CoV-2 and MERS-CoV, H5N1, COX-A9 and HSV1 viruses.

3.13. Electron microscopic examination

Transmission electron microscope (TEM) examination was done for influenza A/H5N1 virus before and after LRD treatment and after the concentration of the virus samples.

3.14. Statistical analysis

Statistical quantitative analysis was done using ANOVA with Tukey's multiple comparison tests to compare between more than two groups and the significance level was evaluated at $p < 0.05$.

4. Results

4.1. Scientific theory of LRD

As shown in Figure 1 and Figure 2, the design of the LRD device **depended** on the energy source from dry batteries. The produced energy will be electronically processed to the codified **number** of ions. The electric stimulation is coded to destroy the biological contents of viruses such as RNA/DNA or the outer envelope.

4.2. Plaque infectivity assay

4.2.1. MERS-CoV virus

The *in vitro* plaque assays demonstrated **a significant** reduction in the viral load of MERS-CoV (Figure 3A). Quantitatively, the treatment with LRD reduced the infectious titer of the MERS-CoV virus to 83% after 30 min and 21% after 1 h compared to the control virus without treatment (Figure 3B). This data indicates that electric stimulation produced by LRD might affect the biological contents of the MERS-CoV virus. Additionally, as shown in table 1, the percentage of viral inhibition after 30 min and 60 min was 15.8 and 78.3 respectively.

4.2.2. COX-A9 virus

As shown in figure 4 the plaque assay showed a significant reduction of the viral load of COX-A9 post 30 min or 60 min exposure to the LRD (Figure 4A). The quantitative analysis of the viral count after 30 min treatment with the LRD showed a decrease in the viral count into 98.7% compared with the non-treated virus. While COX-A9 virus exposure for 60 min exterminates 100% of the virus (Figure 4B). This data indicated that viral exposure to LRD exterminate the dominant of the COX-A9 virus in a short time. Table 2 showed that the inhibition percentage of COX-A9 virus

after 30 min and 60 min of treatment with the LRD was 99.7 and 99.9, respectively.

4.2.3. HSV1 virus

The HSV1 virus infectivity significantly reduced after treatment with LRD as shown from the plaques assay test (Figure 5A and Table 3). The quantitative analysis of the HSV1 viral count showed a 77.7% decrease in the viral count after 30 min exposure to LRD. Viral exposure into LRD for 60 min reduced the number of HSV1 to 84.12% compared with non-treated samples (Figure 5B). The reduction of the viral count of non-enveloped HSV1 virus confirmed the efficacy of LRD to reduce either the enveloped or non-enveloped viral infectivity.

4.2.4. SARS-CoV-2 virus

The experiments of plaque infectivity assay showed a highly significant reduction in viral loads of SARS-CoV-2 (Figure 6A and Table 4). The titration assay showed that the reduction of the propagated viral load reduced into 22% and 1% of the original concentration of the no-treated virus. The infectivity reduction ratio of the SARS-CoV-2 virus is inconsistent with that of MERS-CoV after treatment with LRD. This data indicated that the codified number of ions produced by LRD might specifically affect respiratory viruses.

4.3. The efficacy of LRD against viral load inhibition

The reduction of propagated SARS-CoV-2 viral load using frequencies produced by LRD rather than precipitate produced in the viral media was investigated using two different metal rods of LRD. Both nickel-coated copper (Figure 4A) and iron-copper-coated (Figure 6B and Table 4) rods produced the same ratio of the viral load inhibition. In this experiment, the viral load inhibition of SARS-CoV-2 reduced to 21% and 1% after 30 min and 60 min respectively of the treatment with LRD compared with the non-

treated propagated virus (Figure 6). This experiment The non-significant change in viral load inhibition of SARS-CoV-2 virus after metal rod change indicated that **the codified number** of ions specifically destroy the biological materials of the virus. Additionally, non-of both types of rods (nickel-coated copper or nickel-coated iron) **affect on** the viral load or the formation of the precipitate observed or change in the media pH. This experiment was repeated **three times** (n = 3) for reproductively. This data indicated that the antiviral activity against SARS-CoV-2 is due to the codified **number** of ions generated by the LRD but not from the effect of the chemical precipitate.

4.4. Ultrastructural abnormalities in H5N1 virus

To investigate the effect of LRD treatment on the internal contents of the H5N1 virus, the treated and non-treated H5N1 virus was processed and investigated under transmission electron microscopy. The cellular membrane and nucleic materials of the treaded virus with LRD were seen degenerated and apoptotic under electron microscopy (Figure 7A and 7B). Additionally, we observed that the number **of virus** under the transmission electron microscope decreased after being treated with LRD compared with the non-treated virus. These data indicated that the codified **number** of ions produced by LRD might destroy the biological materials of the H5N1 virus. This data was inconsistent with the data of the plaque infertility assay mentioned in Figure 3 and Figure 6.

4.5. Viral nucleic acid material examination

To confirm the destruction of the nucleic acid materials of treated viruses with LRD, the amount of nucleic acid proteins was quantified using gel electrophoresis. The nucleic acid materials of the H5N1 and MERS-CoV viruses appeared at 55-70 kDa. As shown in Figure 8, the amount of nucleic materials of the treated H5N1 reduced significantly compared with that of the non-treated virus. From another hand, the treated MERS-CoV showed a significant decrease in the nucleic acid amount of the treated virus compared

with the non-treated virus with LRD. The nucleic acids of the cultivated cell lines (MDCK and VERO) were not affected by the treatment of LRD. The data of H5N1 and MERS-CoV protein analysis using electrophoretic patterns confirmed the reduction of viral infectivity using the plaque assay test.

5. Discussion

Recently, the treatment and protection of human viruses caused by SARS-CoV-2, MERS-CoV, H5N1 COX-A9, and HSV1 viruses is a great challenge. For example, In March 2021 WHO announced that the COVID-19 pandemic caused more than 126 million confirmed infected cases and 2 million deaths.²⁴ The current therapies of protection or even treatment of the side effects produced by viral infection using vaccination or antiviral drugs respectively is not completely ideal based on WHO standards. Therefore, it is important to develop standard therapy to reduce viral side effects or infectivity with low cost, painless and lower side effects. Because of conformational changes in proteins on the viral capsid, viruses will subsequently reduce their ability to infect cells. These proteins require energy to activate the chemical reaction that leads to the conformational change in order to undergo a conformational change. The generation of virus mutants that are resistant to such drugs, a low potency in vivo, and toxic side effects are all major issues in the development of effective entry inhibitors. Despite the fact that rapid progress in our understanding of the structural mechanisms of virus entry promises new discoveries, approaches capable of 'outwitting' the virus, no entry clinically used inhibitors or treatment protocols have far been developed on the basis of forecasts by structural models, and the primary source of new information inhibitors are still discovered by screening large libraries of small molecules.

The papered LRD system in this study depends on the production of the codified number of ions that can exterminate the biological materials of the treated viruses.^{15,25,26} Interestingly, stimulation of auricular vagus nerve by

electric frequencies reduced the side effects of lung inflammations caused by SARS-CoV-2.²⁵ Additionally, patients infected with human immunodeficiency virus type 1 (HIV-1) exposed to low electric potential frequencies showed minimal side effects and reduction of the viral infectivity.^{16,26} Interestingly, the previous reports are consistent with our hypothesis about viral infectivity reduction using the codified **number** of ions produced by LRD.

In this study, the pneumonia virus's (SARS-CoV-2, MERS-CoV, H5N1) infectivity ratio decreased significantly due to exposure to the codified **number** of ions produced by LRD. For example, the respiratory virus's treatment with LRD reduced the infectious titer of the MERS-CoV virus to 83% after 30 min and 21% after 60 min. Additionally, the treatment of the SARS-CoV-2 virus reduced the viral propagation to 22% and 1% of the viral original concentration. To confirm the efficacy of the LRD, COX-A9 and HSV1 viruses were exposed to LRD for 30 min and the viruses were exterminated into 98% and 79% respectively. Additionally, we emphasized that the codified **number** of ions produced from LRD are responsible to reduce the SARS-CoV-2 viral load but not the precipitate produced by metal rods used in the LRD. This data is consistent with previously published data about the effect **of electric stimulation on viral** infectivity.^{15,25,26} The mechanism of how electric stimulation reduces the infectivity of respiratory viruses is still unclear. It is expected that the specificity of the viral envelope to the low codified **number** of ions produced by LRD is higher than that of the infected plasma membrane cells. This hypothesis is confirmed with previously published studies about the effect of electric stimulation on the cell membrane or viral envelope fluidity.^{27,28} A previous study reported that electric simulations and anesthetic xylocaine reduced the cell membrane fluidity, in turn affecting HIV-1 infectivity.^{27,28} There was a big difference between the thickness, function and structure of the viral envelope and eukaryotic cell plasma membrane. It is well known that the viral envelope thickness measured 6.34 ± 0.49 nm and was composed of lipid bilayer²⁹. while the plasma membrane

thickness of the eukaryotic cells was measured from 5 nm to 10 nm and composed from phospholipid bilayer, glycoproteins and glycolipids.³⁰ It was hypothesized that the lower potential sensitivity of HIV-1 would be higher than that of infected cells, and this is because the fluidity of the viral envelope is significantly lower than that of the plasma cell membrane.²⁸ It is well known that cell membrane fluidity and lipid bilayer density affects cell functions.^{31,32} Therefore, the codified **number** of ions produced by LRD can specifically destroy the viral envelope and deeper into the nucleic acid materials rather than the infected cells. This data confirms that LRD considers an alternative therapy with lower side effects and is safe for normal cells.

The main purpose of LRD design is to reduce viral or bacterial infectivity as well as the antibacterial and antiviral drugs side effects. For example, common antibiotics have many drug side effects such as digestive system disruption, hematological disorders, organ function failure, cardiac problems, allergic stimulations and longtime neuropathy from fluoroquinolone antibiotics.³³ From another hand, direct-acting antiviral drugs for many **virus diseases** treatments carries the highest category warnings from Food and Drug Administration organization.³⁴ This study showed **the destruction of** the nucleic acid materials of the treated viruses compared with non-treated viruses or the infected cells. This data indicates that **LRD affects specifically** the biological materials (envelope and nucleic acids) of the viruses. Additionally, it was reported previously that the destruction of virus biological materials might occur using the produced nitric oxide and reactive oxygen species (ROS) by electric stimulation.¹³ Therefore, electric stimulation plays a role in cardiac differentiation of human embryonic stem cells, through mechanisms associated with the intracellular generation of ROS.³⁵

Conclusion

Pneumonia virus's treatment or protection with lower side effects is a great challenge. Recently, a non-invasive and alternative therapy is the most suitable strategy for respiratory viral infection treatment. The obtained results from this study showed a high inhibition effect of LRD on the MERS-CoV, SARS-CoV-2 and H5N1 viruses through one-hour treatment. The virus infectivity inhibition effect was observed on nucleic acid materials reduction of enveloped Pneumonia viruses. Interestingly, the DNA and RNA genome are affected much due to LRD treatment. The destruction of the nucleic materials of the viruses by LRD it might due to the codified number of ions specifically to the viral envelope fluidity. We showed in this study that, the efficacy of a codified number of ions produced by LRD is effective to reduce the viral load of SARS-CoV-2 but not the precipitate formation from metal rods observed in the viral media. The data of this study is helpful to design an alternative therapy for viral infectivity reduction in the infected respiratory channels. Additionally, this type of novel treatment saves safe and will reduce the side effects of the antiviral drugs therapy.

Ethics approval and consent to participate

All experiments are performed according to the ethical guidelines for the use of cell lines and approved by animal care and maintenance in the National Research Centre, Cairo, Egypt.

References

1. Leal Ede S, Zanotto PM. Viral diseases and human evolution. Mem Inst Oswaldo Cruz. 2000;95 Suppl 1:193-200. doi: 10.1590/s0074-02762000000700033.
2. Simmonds P, Aiewsakun P. Virus classification - where do you draw the line?. Arch Virol. 2018;163(8):2037-2046. doi:10.1007/s00705-018-3938-z.
3. Shi T, Arnott A, Semogas I, Falsey AR, Openshaw P, Wedzicha JA, Campbell H, Nair H; RESCEU Investigators. The Etiological Role of

Common Respiratory Viruses in Acute Respiratory Infections in Older Adults: A Systematic Review and Meta-analysis. *J Infect Dis.* 2020;222(Supplement_7):S563-S569. doi: 10.1093/infdis/jiy662.

4. Peiris M. Pathogenesis of avian flu H5N1 and SARS. *Novartis Found Symp.* 2006;279:56-60; discussion 60-5, 216-9.

5. Hoheisel G, Luk WK, Winkler J, Wirtz H, Gillissen A, Hui DS, Liebert UG. Aviäre Influenza und das Schwere Akute Respiratorische Syndrom (SARS) - Erfahrungen und Perspektiven [Avian influenza and the Severe Acute Respiratory Syndrome (SARS) - experiences and perspectives]. *Pneumologie.* 2007;61(1):41-5. German. doi: 10.1055/s-2006-955002.

6. Chutinimitkul S, Payungporn S, Chieochansin T, Suwannakarn K, Theamboonlers A, Poovorawan Y. The spread of avian influenza H5N1 virus; a pandemic threat to mankind. *J Med Assoc Thai.* 2006;89 Suppl 3:S218-33.

7. Dhakal BP, Sweitzer NK, Indik JH, Acharya D, William P. SARS-CoV-2 Infection and Cardiovascular Disease: COVID-19 Heart. *Heart Lung Circ.* 2020;29(7):973-987. doi: 10.1016/j.hlc.2020.05.101.

8. Bleibtreu A, Bertine M, Bertin C, Houhou-Fidouh N, Visseaux B. Focus on Middle East respiratory syndrome coronavirus (MERS-CoV). *Med Mal Infect.* 2020;50(3):243-251. doi: 10.1016/j.medmal.2019.10.004.

9. Moreau B, Bastedo C, Michel RP, Ghali P. Hepatitis and Encephalitis due to Coxsackie Virus A9 in an Adult. *Case Rep Gastroenterol.* 2011 Sep;5(3):617-22. doi: 10.1159/000333135.

10. Whitley RJ. Herpes simplex virus infection. *Semin Pediatr Infect Dis.* 2002 Jan;13(1):6-11. doi: 10.1053/spid.2002.29752. PMID: 12118847.

11. Fraser CS, Jha A, Openshaw PJ. Vaccines in the Prevention of Viral Pneumonia. *Clin Chest Med.* 2017;38(1):155-169. doi: 10.1016/j.ccm.2016.11.009.
12. Razonable RR. Antiviral drugs for viruses other than human immunodeficiency virus. *Mayo Clin Proc.* 2011;86(10):1009-1026. doi:10.4065/mcp.2011.0309.
13. Hart H, Reid K, Hart W. Inactivation of viruses during ultraviolet light treatment of human intravenous immunoglobulin and albumin. *Vox Sang.* 1993;64(2):82-8. doi: 10.1111/j.1423-0410.1993.tb02523.x.
14. Roberts P, Hope A. Virus inactivation by high intensity broad spectrum pulsed light. *J Virol Methods.* 2003;110(1):61-5. doi: 10.1016/s0166-0934(03)00098-3.
15. Kumagai E, Tominaga M, Nagaishi S, Harada S. Effect of electrical stimulation on human immunodeficiency virus type-1 infectivity. *Appl Microbiol Biotechnol.* 2007;77(4):947-53. doi: 10.1007/s00253-007-1214-3.
16. Kumagai E, Tominaga M, Harada S. Sensitivity of chronically HIV-1 infected HeLa cells to electrical stimulation. *Appl Microbiol Biotechnol.* 2004;63(6):754-8. doi: 10.1007/s00253-003-1410-8.
17. Tominaga M, Kumagai E, Harada S. Effect of electrical stimulation on HIV-1-infected HeLa cells cultured on an electrode surface. *Appl Microbiol Biotechnol.* 2003;61(5-6):447-50. doi: 10.1007/s00253-003-1225-7.
18. Ilawadhi P, Khurana A, Allwadhi S, Navik US, Joshi K, Banothu AK, Bharani KK. Potential of electric stimulation for the management of COVID-19. *Med Hypotheses.* 2020;144:110259. doi:10.1016/j.mehy.2020.110259.
19. Xue J, Chambers BS, Hensley SE, López CB. Propagation and Characterization of Influenza Virus Stocks That Lack High Levels of

Defective Viral Genomes and Hemagglutinin Mutations. *Front Microbiol.* 2016;7:326. doi:10.3389/fmicb.2016.00326.

20. Karakus U, Cramer M, Lanz C, Yángüez E. Propagation and Titration of Influenza Viruses. *Methods Mol Biol.* 2018;1836:59-88. doi: 10.1007/978-1-4939-8678-1_4.

21. Mendoza EJ, Manguiat K, Wood H, Drebot M. Two Detailed Plaque Assay Protocols for the Quantification of Infectious SARS-CoV-2. *Curr Protoc Microbiol.* 2020;57(1):ecpmc105. doi: 10.1002/cpmc.105.

22. Hayden, F.G., Cote, K.M., Douglas, R.G. Plaque inhibition assay for drug susceptibility testing of influenza viruses. *Antimicrob. Agents Chemother.*; 1980;17, 865-870.

23. Morrissey JH. Silver stain for proteins in polyacrylamide gels: a modified procedure with enhanced uniform sensitivity. *Anal Biochem.* 1981;117(2):307-10. doi: 10.1016/0003-2697(81)90783-1.

24. Perico L, Benigni A, Casiraghi F, Ng LFP, Renia L, Remuzzi G. Immunity, endothelial injury and complement-induced coagulopathy in COVID-19. *Nat Rev Nephrol.* 2021;17(1):46-64. doi: 10.1038/s41581-020-00357-4.

25. Kaniusas E, Szeles JC, Kampusch S, Alfageme-Lopez N, Yucuma-Conde D, Li X, Mayol J, Neumayer C, Papa M, Panetsos F. Non-invasive Auricular Vagus Nerve Stimulation as a Potential Treatment for Covid19-Originated Acute Respiratory Distress Syndrome. *Front Physiol.* 2020;11:890. doi: 10.3389/fphys.2020.00890.

26. Kumagai E, Tominaga M, Harada S. Sensitivity to electrical stimulation of human immunodeficiency virus type 1 and MAGIC-5 cells. *AMB Express.* 2011;1(1):23. doi:10.1186/2191-0855-1-23

27. Kojima J, Shinohara H, Ikariyama Y, Aizawa M, Nagaike K, Morioka S. Electrically controlled proliferation of human carcinoma cells cultured on the surface of an electrode. *J Biotechnol.* 1991;18(1-2):129-39. doi: 10.1016/0168-1656(91)90241-m.
28. Harada S, Yusa K, Monde K, Akaike T, Maeda Y. Influence of membrane fluidity on human immunodeficiency virus type 1 entry. *Biochem Biophys Res Commun.* 2005;329(2):480-6. doi: 10.1016/j.bbrc.2005.02.007.
29. Hawes PC, Netherton CL, Wileman TE, Monaghan P. The envelope of intracellular African swine fever virus is composed of a single lipid bilayer. *J Virol.* 2008 Aug;82(16):7905-12. doi: 10.1128/JVI.00194-08.
30. Nicolson GL. Update of the 1972 Singer-Nicolson Fluid-Mosaic Model of Membrane Structure. *Discoveries (Craiova).* 2013;1(1):e3. Published 2013 Dec 31. doi:10.15190/d.2013.3
31. Lande MB, Donovan JM, Zeidel ML. The relationship between membrane fluidity and permeabilities to water, solutes, ammonia, and protons. *J Gen Physiol.* 1995;106(1):67-84. doi: 10.1085/jgp.106.1.67.
32. Muller CP, Volloch Z, Shinitzky M. Correlation between cell density, membrane fluidity, and the availability of transferrin receptors in Friend erythroleukemic cells. *Cell Biophys.* 1980;2(3):233-40. doi: 10.1007/BF02790451.
33. Heta S, Robo I. The Side Effects of the Most Commonly Used Group of Antibiotics in Periodontal Treatments. *Med Sci (Basel).* 2018;6(1):6. doi:10.3390/medsci6010006
34. Vcev A. Terapija nuspojava antivirusne terapije [Management of side effects during antiviral therapy]. *Acta Med Croatica.* 2009;63(5):463-7. Croatian.

35. Serena E, Figallo E, Tandon N, et al. Electrical stimulation of human embryonic stem cells: cardiac differentiation and the generation of reactive oxygen species. *Exp Cell Res.* 2009;315(20):3611-3619. doi:10.1016/j.yexcr.2009.08.015.

Figure legends

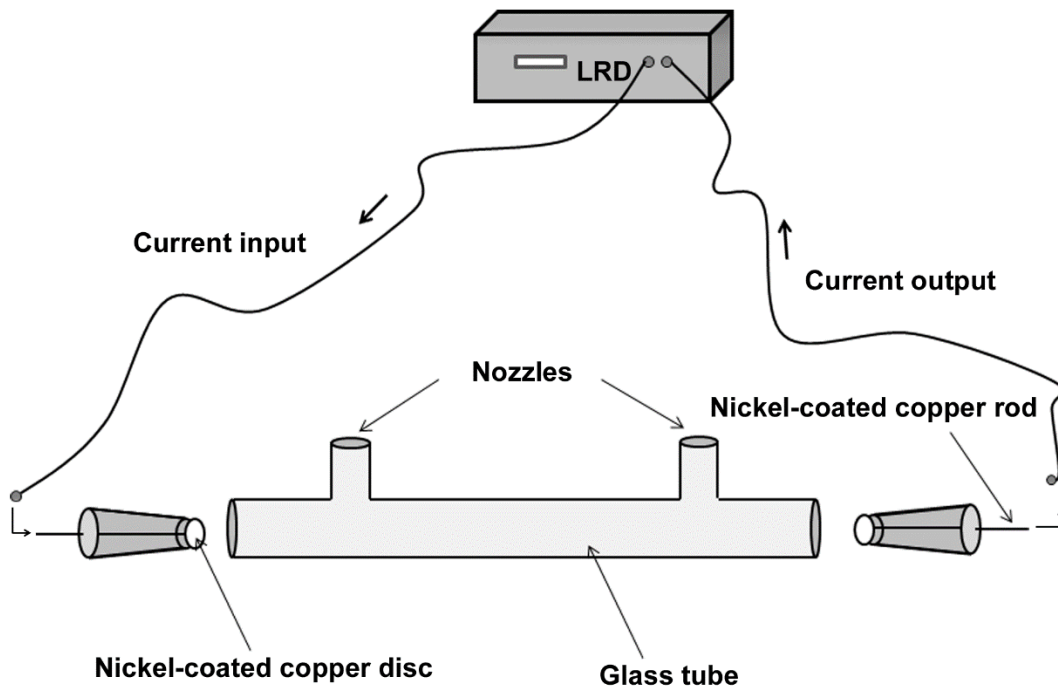


Figure 1: Diagrammatic graph showing the in vitro experiment design. The glass tube will be filled with cell culture medium and virus. Then the two ends of nickel-coated copper rods will be connected with the LRD. The electric stimulation will be produced and controlled through the by LRD.

A



B

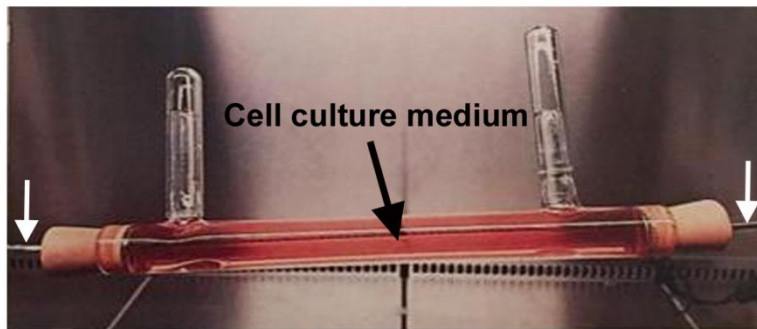


Figure 2: (A), A photo of primary model of LRD showing the controller (white arrow) for electric stimulation production. (B), A designed glass tube filled with cell culture medium and targeted virus. The glass tube will be connected with the LRD through the input and output power sources (white arrow).

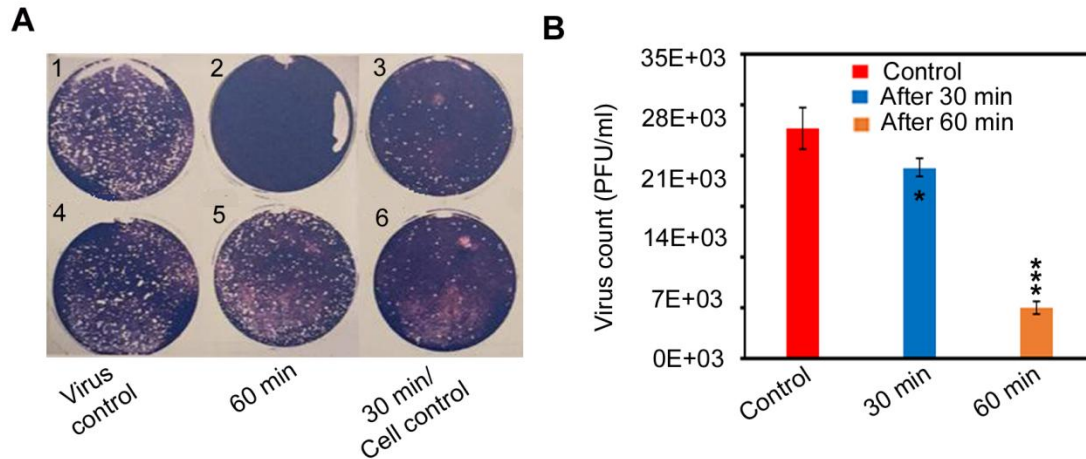


Figure 3: (A) Plaque assay titration of MERS-CoV before and after treatment with LRD for 30 min and 60 min. (B) Quantitative analysis of MERS-CoV after treatment with LRD. Note: 1 and 4 = virus control; 2 and 5 = after 60 min; 3 = after 30 min; 6 = cell control. * and *** indicate p value of < 0.01 and < 0.001 , respectively (ANOVA with Tukey's multiple comparison test). Number of trials is 3 times ($n = 3$).

Trial no.	Initial virus conc. (PFU/ml)	Exposure time	Virus conc. (PFU/ml) after treatment	Percent of virus inhibition (%)
1	3.2×10^4	30 min	2.6×10^4	18.75
		60 min	7×10^3	78
2	3.5×10^4	30 min	2.5×10^4	28.75
		60 min	8×10^3	77
3	2.8×10^4	30 min	2.8×10^4	0
		60 min	5.7×10^3	79.6
Average	3.1×10^4	30 min	2.6×10^4	15.8
		60 min	6900	78.3
SD	2867	30 min	1247	11.9
		60 min	941	1.03

Table 1: Plaque assay titration of MERS-CoV virus before and after treatment with LRD for 30 min and 1 hr. Number of trials is 3 times (n = 3).

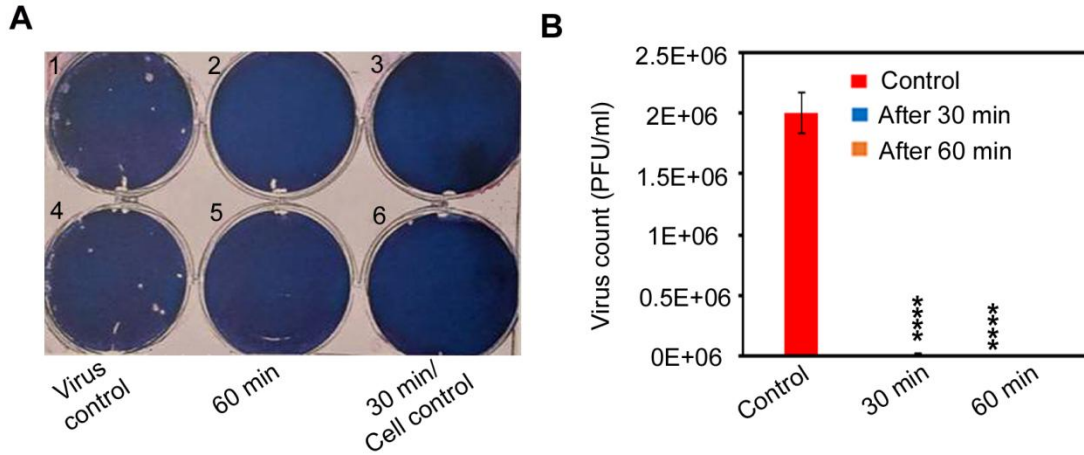


Figure 4: (A) Plaque assay titration of COX-A9 before and after treatment with LRD for 30 min and 60 min. (B) Quantitative analysis of HSV1 after treatment with LRD. Note: 1 and 4 = virus control; 2 and 5 = after 60 min; 3 = after 30 min; 6 = cell control. *** and **** indicate p value of < 0.001 and < 0.0001 , respectively (ANOVA with Tukey's multiple comparison test). Number of trials is 3 times ($n = 3$).

Trail no.	Initial virus conc. (PFU/ml)	Exposure time	Virus conc. (PFU/ml) after treatment	Percent of virus inhibition (%)
1	2×10^6	30 min	2.6×10^4	98.7
		60 min	0	100
2	2.2×10^6	30 min	2.8×10^4	98.7
		60 min	200	99.9
3	1.8×10^6	30 min	2.5×10^4	98.6
		60 min	500	99.9
Average	2×10^6	30 min	2.6×10^4	99.7
		60 min	233	99.9
SD	1.6×10^5	30 min	1247	0.04
		60 min	205	0.01

Table 2: Plaque assay titration of COX-A9 virus before and after treatment with LRD for 30 min and 1 hr. Number of trials is 3 times (n = 3).

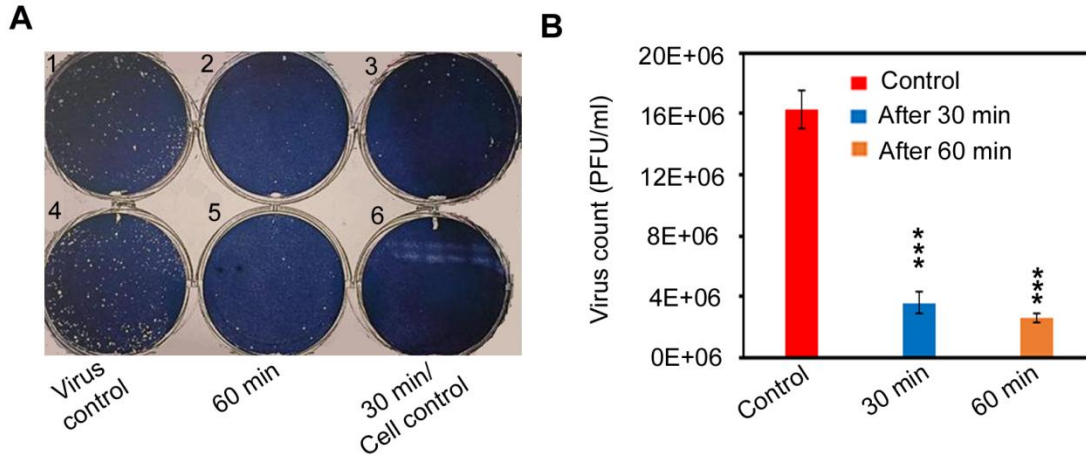


Figure 5: (A) Plaque assay titration of HSV1 before and after treatment with LRD for 30 min and 60 min. (B) Quantitative analysis of HSV1 after treatment with LRD. Note: 1 and 4 = virus control; 2 and 5 = after 60 min; 3 = after 30 min; 6 = cell control. *** indicate p value of < 0.001 (ANOVA with Tukey's multiple comparison test). Number of trials is 3 times (n = 3).

Trial no.	Initial virus conc. (PFU/ml)	Exposure time	Virus conc. (PFU/ml) after treatment	Percent of virus inhibition (%)
1	16×10^6	30 min	3.4×10^6	78.75
		60 min	2.5×10^6	84.3
2	18×10^6	30 min	2.8×10^6	84.4
		60 min	3×10^6	83.3
3	15×10^6	30 min	4.5×10^6	70
		60 min	2.3×10^6	84.7
Average	16.3×10^6	30 min	3.56×10^6	77.73
		60 min	2.6×10^6	84.12
SD	$1.24.3 \times 10^6$	30 min	7×10^5	5.94
		60 min	2.9×10^5	0.57

Table 3: Plaque assay titration of HSV1 virus before and after treatment with LRD for 30 min and 1 hr. Number of trials is 3 times (n = 3).

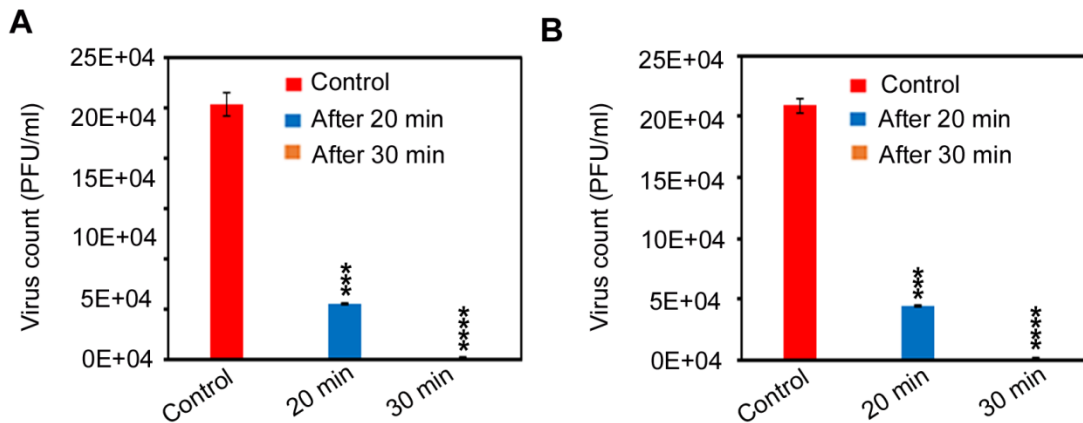


Figure 6: (A) Quantitative analysis of SARS-CoV-2 (COVID-19) inhibition before and after treatment with LRD for 20 min and 30 min using nickel-coated copper rod. During the experiment, we observed a change in the pH of virus-containing medium and this change was associated with chemical white precipitation. (B) Quantitative analysis of SARS-CoV-2 (COVID-19) inhibition before and after treatment with LRD for 20 min and 30 min using nickel-coated iron rod. During the experiment, we observed a change in the pH of virus-containing medium (black) and this change was associated with chemical black precipitation. *** and **** indicate p value of < 0.001 and < 0.0001 , respectively (ANOVA with Tukey's multiple comparison test). Number of trials is 3 times ($n = 3$).

Trail no.	Rod type	Initial virus conc. (PFU/ml)	Exposure time	Virus (PFU/ml) treatment	conc. after	Percent virus inhibition (%)	of
1	Nickel-coated copper	2.42x10 ⁵	20 min	5.4x10 ⁴		77.68	
			30 min	1.20x10 ³		99.5	
	Nickel-coated iron	2.42x10 ⁵	20 min	5.3X10 ⁴		78.09	
			30 min	1.22X10 ³		99.49	
2	Nickel-coated copper	2.7x10 ⁵	20 min	5.5x10 ⁴		79.6	
			30 min	2000		99.25	
	Nickel-coated iron	2.5x10 ⁵	20 min	5.4x10 ⁴		78.4	
			30 min	2100		99.16	
3	Nickel-coated copper	2.5x10 ⁵	20 min	5.6x10 ⁴		77.6	
			30 min	3000		98.8	
	Nickel-coated iron	2.6x10 ⁵	20 min	5.5x10 ⁴		78.8	
			30 min	3100		98.8	
Average	Nickel-coated copper	2.5x10 ⁵	20 min	5.5x10 ⁴		78.3	
			30 min	2066		99.18	
	Nickel-coated iron	2.5x10 ⁵	20 min	5.4x10 ⁴		78.4	
			30 min	2140		99.1	
SD	Nickel-coated copper	1.1x10 ⁴	20 min	816		0.93	
			30 min	736		0.3	
	Nickel-coated iron	7363	20 min	816		0.3	
			30 min	768		0.3	

Table 4: Plaque assay titration of SARS-CoV-2 virus before and after treatment with LRD equipped with nickel-coated copper rod or nickel-coated iron rod for 30 min and 1 hr. Number of trials is 3 times (n = 3).

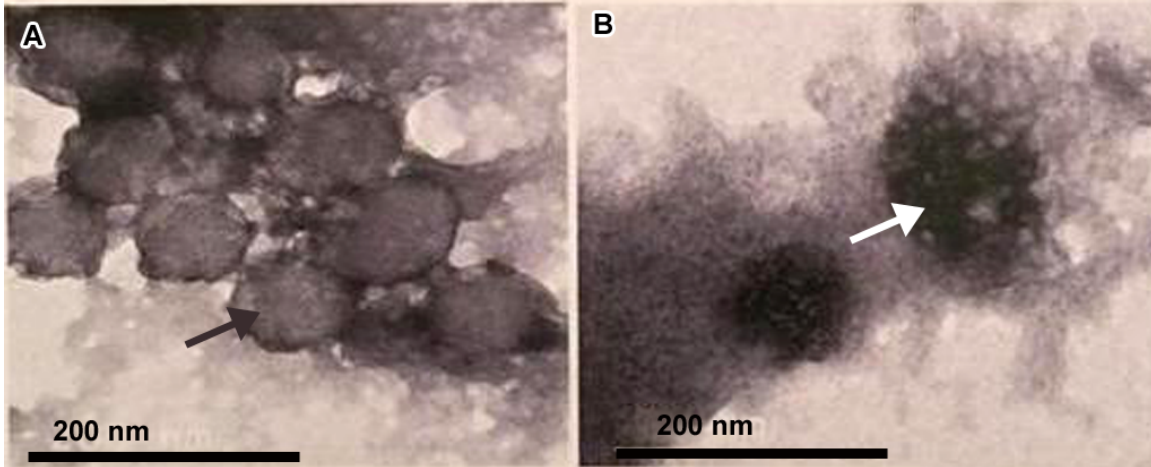


Figure 7: (A) Untreated H5N1 virus under transmission electron microscopy without any abnormalities (black arrow). (B) Treated H5N1 virus with LRD for 60 min showing destroyed cell membrane and vacuolated nucleus of H5N1 virus (white arrow).

UNDER PEER REVIEW

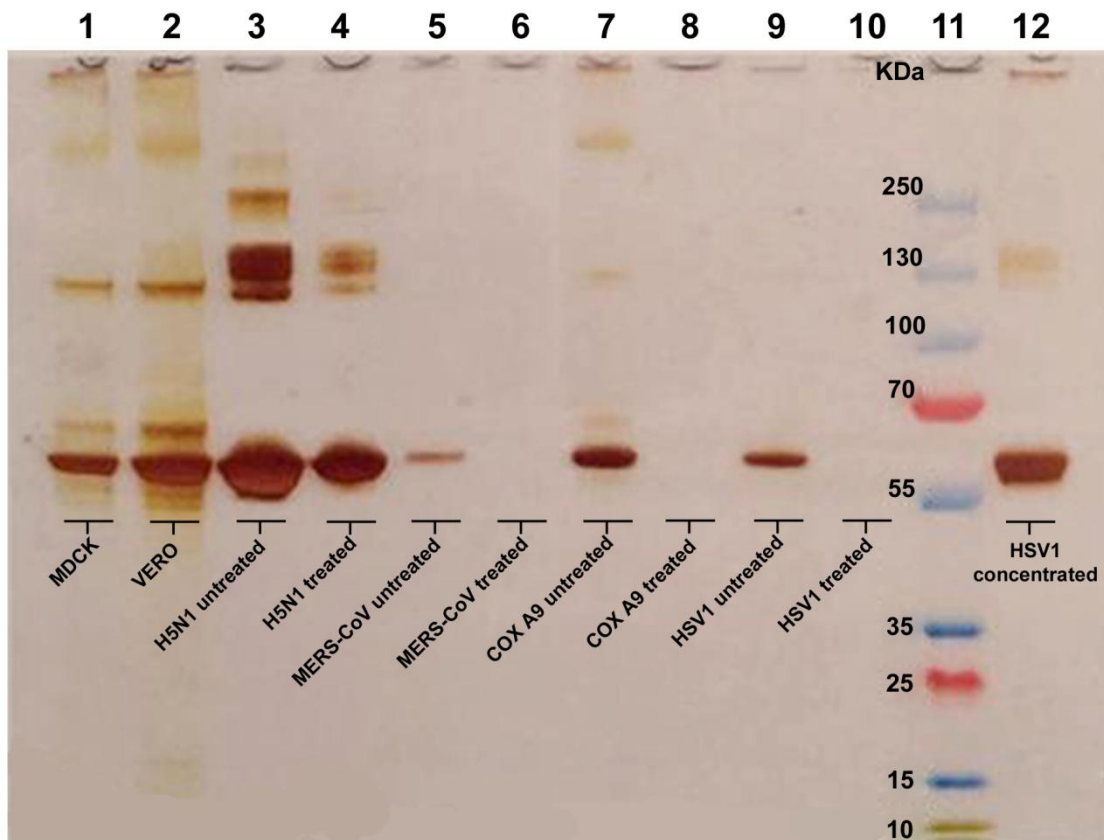


Figure 8: Electrophoretic pattern on gradient SDS-PAGE of different virus's proteins expressed and purified of cell culture after and before treatment with LRD. Note: 1 and 2 panel for MDCK and VERO cells, 3 and 4 panels for H5N1 virus before and after treatment respectively with LRD, 5 and 6 panels for MERS-CoV before and after treatment respectively with LRD, 7 and 8 panels for Cox-A9 before and after treatment respectively with LRD, 9 and 10 panels for HSV1 virus before and after treatment, 11 as standard proteins and 12 panel for concentrated HSV1 virus.